Agricultural and Forest Meteorology 149 (2009) 2120–2132

Contents lists available at ScienceDirect

Agricultural and Forest Meteorology

journal homepage: www.elsevier.com/locate/agrformet

Evaluating the potential use of winter cover crops in corn–soybean systems for sustainable co-production of food and fuel

John M. Baker *, Timothy J. Griffis

USDA-ARS & Department of Soil, Water & Climate, University of Minnesota, St. Paul, MN 55108, United States

ARTICLE INFO

Article history:
Received 1 November 2008
Received in revised form 14 March 2009
Accepted 19 May 2009

Keywords:
Cover crops
Rye
Biofuel
Biomass

ABSTRACT

Climate change and economic concerns have motivated intense interest in the development of renewable energy sources, including fuels derived from plant biomass. However, the specter of massive biofuel production has raised other worries, specifically that by displacing food production it will lead to higher food prices, increased incidence of famine, and acceleration of undesirable land use change. One proposed solution is to increase the annual net primary productivity of the existing agricultural land base, so that it can sustainably produce both food and biofuel feedstocks. This might be possible in corn and soybean production regions through the use of winter cover crops, but the biophysical feasibility of this has not been systematically explored. We developed a model for this purpose that simulates the potential biomass production and water use of winter rye in continuous corn and corn–soybean rotations. The input data requirements represent an attempt to balance the demands of a physically and physiologically defensible simulation with the need for broad applicability in space and time. The necessary meteorological data are obtainable from standard agricultural weather stations, and the required management data are simply planting dates and harvest dates for corn and soybeans. Physiological parameters for rye were taken from the literature, supplemented by experimental data specifically collected for this project. The model was run for a number of growing seasons for 8 locations across the Midwestern USA. Results indicate potential rye biomass production of 1–8 Mg ha^{-1}, with the lowest yields at the more northern sites, where both PAR and degree-days are limited in the interval between fall corn harvest and spring corn or soybean planting. At all sites rye yields are substantially greater when the following crop is soybean rather than corn, since soybean is planted later. Not surprisingly, soil moisture depletion is most likely in years and sites where rye biomass production is greatest. Consistent production of both food and biomass from corn/winter rye/soybean systems will probably require irrigation in many areas and additional N fertilizer, creating possible environmental concerns. Rye growth limitations in the northern portion of the corn belt may be partially mitigated with aerial seeding of rye into standing corn.

Published by Elsevier B.V.

1. Introduction

The increasing recognition of the atmospheric impact of fossil fuel combustion has spurred research and development of renewable alternatives, particularly fuels derived from freshly produced biomass. Ethanol has been the most publicized biofuel to this point, primarily because it can be easily produced from plant-derived sugars and starches and can be used in internal combustion engines with minor modifications. All major ethanol plants in the USA currently use corn grain as their carbon source. However, this constrains capacity to a small fraction of total US fuel consumption, and places energy production in competition with food production for raw material.

Long-anticipated technological improvements may eventually lead to cost-competitive energy production from non-grain biomass, but this will not alleviate food versus fuel concerns if it results in displacement of grain crops with dedicated bioenergy crops such as switch grass, miscanthus, and hybrid poplar. Meeting the ambitious goals that have been set for bioenergy production without impacting food production and without massive land use change is a tremendous challenge. Some have suggested that this can be done with prairie establishment on degraded agricultural lands (Tilman et al., 2006), but others feel that this potential pool is not nearly as large as has been proposed (Russelle et al., 2007). It may be one part of a set of solutions, or one piece of the pie, to borrow the analogy that Pacala and Socolow (2004) have applied to the related issue of stabilizing atmospheric CO_2 levels, but other sustainable, food-neutral sources remain to be identified. Here we explore one potential contributor – greatly increased use of winter cover crops in existing agricultural systems.

* Corresponding author.
E-mail address: John.Baker@ars.usda.gov (J.M. Baker).

0168-1923/$ – see front matter. Published by Elsevier B.V.
doi:10.1016/j.agrformet.2009.05.017

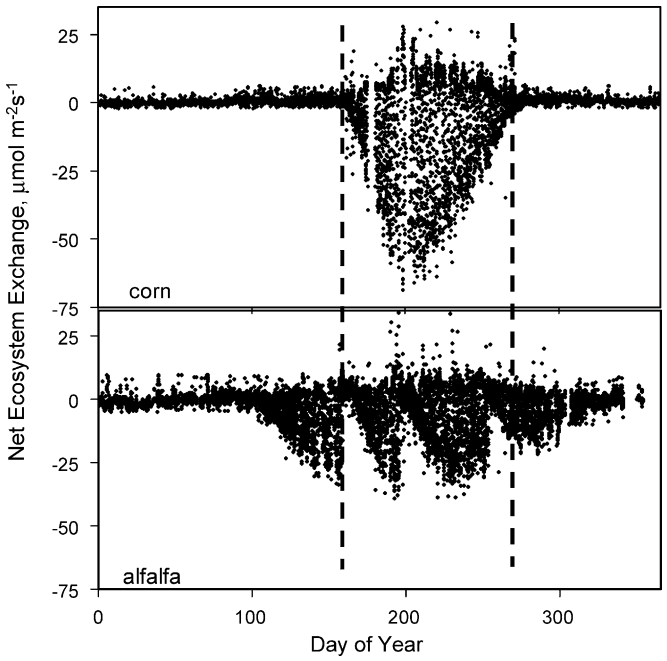

Fig. 1. Half-hourly eddy covariance measurements of net ecosystem exchange of CO_2 for corn and alfalfa at Rosemount and Willmar, MN. Vertical dashed lines delineate the growing season for the corn crop.

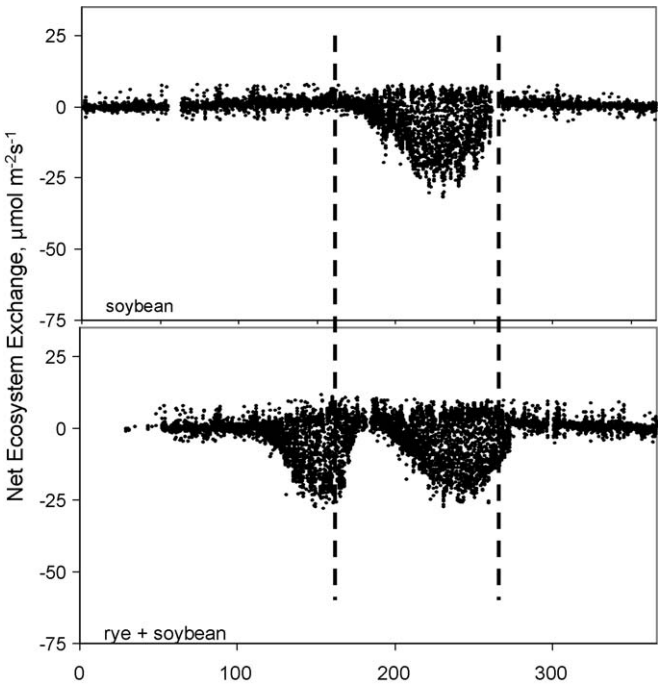

Fig. 2. Half-hourly eddy covariance measurements of net ecosystem exchange of CO_2 for adjacent fields in Rosemount, MN, one a conventionally planted soybean field, the other soybean following a winter rye cover crop. Vertical dashed lines delineate the growing season for the conventional soybean crop.

This approach represents a modification of existing farming systems so that they more efficiently use the solar radiation annually available to them to create additional biomass – to get more carbon into the system before taking more out. Under the warm, high-irradiance conditions prevalent in midsummer in the Midwestern United States, corn fields are capable of net assimilation rates as high or higher than any reported temperate zone ecosystems in the world. And yet, despite this exceptional peak photosynthetic capacity, the annual net primary productivity of a corn/soybean rotation is roughly the same as that of native perennial ecosystems in the same region that have much lower maximum photosynthetic rates (Prince et al., 2001; Schmid et al., 2000). The reason for this is evident in Fig. 1, where we have plotted half-hourly rates of NEE for corn (*Zea mays* L.) and a perennial species, alfalfa (*Medicago sativa* L.), both measured in southern Minnesota, USA. The high mid-season productivity of corn is apparent, but so is its brief lifespan. Net assimilation only lasts for about 105 days (soybean is even more ephemeral, with net carbon uptake lasting approximately 90 days). The perennial alfalfa, on the other hand, begins extracting CO_2 from the atmosphere in this region on about day of year (DOY) 105 and continues until approximately DOY 315, a growing season that is twice as long as either annual crop. As Baldocchi (2008) has recently noted, the most productive ecosystems are those with long growing seasons, rather than high peak productivity.

One possible way to contribute to prospective bioenergy needs *and* continue to meet the demand for food and feed in a sustainable manner is to take advantage of *both* the peak summer efficiency of C4 corn, and the broader, spring-fall capabilities evident in perennial C3 systems through the inclusion of cover crops. There are a number of cover crops that are well adapted to the cooler conditions that prevail in the spring and fall. Some do not overwinter, and hence would be useful as either spring or fall crops, but not both. Others, such as winter wheat (*Triticum aestivum* L.) and rye (*Secale cereale* L.) can survive even the harsh winters of the northern Corn Belt, and thus could assimilate C in both the fall and the following spring. Winter rye has been extensively tested as a cover crop in corn/soybean rotations (Ruffo et al., 2004; Coelho et al., 2005; Feyereisen et al., 2006a,b; Kaspar et al., 2007). It is sometimes planted following corn harvest, then killed just before planting of soybean or corn the succeeding spring. We have measured NEE continuously in such a farming system for several years at Rosemount, MN, USA (Baker and Griffis, 2005). Half-hourly data from an entire year are shown in the lower panel of Fig. 2. Comparison with a nearby conventional soybean field (upper panel) reveals substantial additional C assimilation in the cover cropped system. The accumulated rye biomass in this system was nearly 5 Mg ha^{-1}, but to accomplish this it was necessary to allow the rye to continue growing for several weeks after the succeeding soybean crop was planted, and this ultimately had a negative effect on soybean yield, decreasing it by 15% relative to a control field. It may be possible to maintain the rye production and still remove it early enough to avoid impacts on the following crop if the rye can somehow be planted earlier in the fall. Conventional planting with a grain drill must wait until the preceding corn crop is harvested, but some producers have experimented with helicopter seeding into the standing corn canopy, allowing the rye to germinate and begin vegetative growth prior to corn harvest. We hypothesized that this would increase the amount of rye biomass available for harvest at an earlier point in the spring to minimize effects on the following crop. Furthermore, since an established cover crop also provides erosion protection in the fall and spring, some fraction of the stover from the previous corn crop could probably be sustainably harvested without negative soil erosion or quality effects, a point noted in a recent life-cycle analysis of stover ethanol production (Kim and Dale, 2005). However, it is difficult to draw any conclusions regarding the potential regional or national biomass contributions from winter rye cover crops in corn/soybean systems on the basis of a few isolated field experiments. Also, producers are hesitant to adopt cover cropping without a broader assessment of the potential risks and benefits. In particular, there are concerns that the water used by a winter cover crop will increase the likelihood that the subsequent summer crop will be affected by drought stress. Ideally these questions might be addressed with multi-year field experiments at multiple sites, but

such experiments are difficult to conduct and even more difficult to fund. As a preliminary step, we have developed a model to tentatively address these questions, and to use heuristically to guide further field research. Our specific modeling goals were:

1. To estimate the potential additional biomass that can be produced at locations across the corn belt through the use of winter rye cover cropping.
2. To estimate the additional water use associated with winter rye cover cropping.
3. To estimate how planting date (particularly through aerial seeding into standing corn) and kill date affect the answers to goals 1 and 2.
4. To delineate uncertainties and areas needing further research.

1.1. Constraints

1. The model must be simple and robust, but should be based to the greatest extent possible on sound physical and physiological principles.
2. The model must operate with the meteorological data available from standard agricultural weather network stations, i.e. – temperature, relative humidity, solar radiation, shallow soil temperature, and precipitation.

2. Approach

The model estimates *potential* biomass production and water use of winter rye, i.e. – it assumes no limitations due to water stress or nutrient deficiencies. It scales leaf photosynthesis and transpiration to the canopy with a sun/shade approach (Norman, 1993; dePury and Farquhar, 1997, 1999). A number of physiological parameters must be known or estimated, and management parameters are also required, including harvest date for the previous crop and seeding date for the succeeding crop. The model uses either hourly or half-hourly averages of air temperature, relative humidity, incoming solar radiation, surface layer soil temperature, and precipitation. For any given year, simulation commences at the time of rye seeding in the fall and concludes in late spring of the following year. The fall portion of the model concludes at the time the soil begins freezing, and the spring component commences at the time of soil thawing.

Emergence is estimated as a function of soil growing degree-days, with 100 GDD (0 °C base) required. If the specified seeding date is prior to the harvest date of the previous crop it is assumed that the rye was aerially seeded, i.e. – broadcast by helicopter or airplane. This means that the seed will be sitting on the soil surface, in contrast to seed injected with a grain drill. Under such circumstances, we assume that imbibition does not begin until the first rainfall after planting, so accumulation of GDD does not begin until then. The effective seeding rate, or the fraction of applied seed that produces a plant, is estimated as 85%; certainly it is lower for aerial seeding, but there are insufficient data on which to base a value. We simply assume that once such a number has been established from agronomic experiments, the actual aerial seeding rate will be adjusted upward to produce a plant population equivalent to direct seeding. Upon emergence, the initial leaf area index (LAI) is estimated from the product of the effective seeding rate and the specific leaf area, assuming that 33% of the mass of each germinating seed is converted to leaf tissue.

2.1. Potential assimilation

Potential assimilation denotes the assimilation rate of a non-water stressed canopy with adequate nutrition. Assimilation is estimated separately for sunlit and shaded leaves, with LAI apportioned to sunlit and shaded fractions on the basis of leaf angle distribution, the relative proportions of diffuse and direct beam PAR, and zenith angle (Norman, 1993; Campbell and Norman, 1998). Leaf level photosynthesis is estimated for each fraction using the approach of Collatz et al. (1991), in which net assimilation is computed as the minimum of the light-limited (J_e), rubisco limited (J_c), and sucrose limited (J_s) rates for a given set of ambient conditions, minus respiratory CO_2 production, R_d (Eq. (1)).

$$\begin{aligned} A &= \min[J_e, J_c, J_s] - R_d \\ J_e &= f(\alpha, PAR, c_i, T, P) \\ J_c &= f(c_i, V_m, T, P) \\ J_s &= f(V_m, T) \\ R_d &= f(V_m, T) \end{aligned} \tag{1}$$

α = leaf absorptance for PAR; c_i = CO_2 mole fraction; T = leaf temperature; P = pressure; V_m = Rubisco catalytic capacity.

V_m, the maximum catalytic capacity of rubisco expressed on a leaf area basis, varies with leaf age and leaf position within the canopy, and is strongly correlated with Leaf N content (dePury and Farquhar, 1997). Unfortunately, literature reports of rye photosynthesis parameters are scarce. Winzeler et al. (1989) provide a plot of leaf level assimilation for rye in a growth chamber, presumably provided with adequate nutrition, at 10, 15, 20, and 25 °C under an irradiance of 1300 μmol m^{-2} s^{-1}. Fitting these data to the Collatz model yielded a value for V_m at 25 °C of 90 μmol m^{-2} s^{-1}, with a Q_{10} of 2.1. Yu et al. (2002) reported V_m values of 55–68 μmol m^{-2} s^{-1} for winter wheat, a crop similar in many respects to rye. dePury and Farquhar (1997) found that V_m decreased linearly down through a wheat canopy, directly correlated with N content, from a maximum of about 100 at the top to a minimum of about 60 for the lower leaves. Limited leaf chamber data that we have collected on highly fertilized rye, growing on a soil heavily amended with manure, yielded a V_m of 120 μmol m^{-2} s^{-1} for the uppermost leaves. For the purposes of this numerical exercise, simulations for each site were run with three levels of mean canopy V_m: 65, 80, and 95 μmol m^{-2} s^{-1}, chosen to correspond to poor, moderate, and high soil N availability. Following the dePury and Farquhar example with wheat, R_d was taken to be $0.009V_m$.

The internal CO_2 concentration, c_i, is obtained by iteratively solving Eq. (1), a stomatal action model, and an aerodynamic transport equation. Wong et al. (1979) noted that stomata tend to maintain a stable ratio of internal to external CO_2, c_i/c_s, with values in the range of 0.7 for a broad range of C3 species. Others have since shown that there is a humidity dependence as well, that has been incorporated in a variety of ways (e.g. Collatz et al., 1991; Leuning, 1995). For rye, leaf-level measurements were satisfactorily described by

$$g_s = (1-\varepsilon)^{-1}\frac{A}{c_s} \tag{2}$$

where g_s is stomatal conductance for CO_2, A is assimilation rate, c_s is CO_2 concentration at the leaf surface and $\varepsilon = c_i/c_s$. The latter is a function of PAR and vapor pressure deficit, described in more detail in Appendix A. Transport between the leaf and height z above the canopy is written as

$$A = g_a(c_z - c_s) \tag{3}$$

where c_z is the ambient CO_2 concentration at screen height z, and the aerodynamic conductance g_a is

$$g_a = \frac{k^2 U}{(\ln(z-d/z_0)^2)}\frac{\rho_a}{M_a} \tag{4}$$

in which k is the von Karman constant, U is the wind speed at screen height z, d is the displacement length and z_0 is the roughness length, both taken as functions of crop height, and ρ_a/M_a is the molar density of air. CO_2 mole fraction at z, c_z, is estimated as

$$c_z = c_0 - \Delta \tag{5}$$

where c_0 is the 'free-stream' CO_2 mole fraction, computed from a time series fit of the monthly mean Mauna Loa data (Anon, 2008), and Δ is the near-surface daytime drawdown. The latter is modeled empirically as a function of day of year and solar elevation angle to approximately capture both the seasonal and diurnal variation in regional photosynthetic activity and planetary boundary layer depth:

$$\begin{aligned} c_0 &= 315.45 + .878(\text{year} - 1960) + .0117(\text{year} - 1960)^2 \\ &\quad + 1.46\cos\left(2\pi\frac{DoY - 128}{365}\right) \\ \Delta_c &= \Delta_{\max}\sin\varphi\exp(-.03|DoY - 180|) \end{aligned} \tag{5}$$

Analysis of CO_2 concentration data from the Ameriflux site at Rosemount, MN yielded a value for the maximum mean midday drawdown, $\Delta_{\max}$, of approximately 40 μmol mol^{-1}. Eqs. (1–3) are iteratively solved for both the sunlit and shaded fractions. Canopy assimilation rate is then taken to be the sum of the sunlit and shaded rates, each multiplied by their respective LAI.

2.2. Crop respiration

Respiration has a growth component and a maintenance component McCree (1974). The growth portion is essentially a measure of the efficiency with which photosynthate is converted into plant tissue. This varies among compounds, but a reasonable average conversion efficiency is 70%, i.e. – 30% of photosynthate is consumed during biosynthesis of plant tissue. Maintenance respiration is associated primarily with replacing proteins as they degrade. It is proportional to the total biomass, m_b, and is taken as $.015m_b$ at 20 °C, with a Q_{10} of 2.

2.3. Transpiration

Analogous to assimilation, transpiration (T) is calculated separately for sunlit and shaded fractions, then weighted by the respective leaf area indices and summed. For each fraction,

$$\begin{aligned} T &= k_v(e_c - e_a)P^{-1} \\ k_v &= \left(\frac{1}{g_v} + \frac{1}{g_a}\right)^{-1} \end{aligned} \tag{6}$$

where k_v is the total conductance for water vapor, P is ambient barometric pressure, and $e_c - e_a$ is the vapor pressure gradient between the interior of the leaves and the ambient air. The vapor pressure gradient is estimated from the ambient vapor pressure deficit, on the assumption that the canopy temperature is nearly equal to air temperature. The canopy conductance for water vapor, $g_v = 1.6g_c$ and the aerodynamic conductances for the two scalars are assumed equal.

2.4. Soil evaporation

Soil evaporation is estimated with the Priestley–Taylor equation (Priestley and Taylor, 1972):

$$\lambda E = \alpha\frac{s}{s+\gamma}(Rn - G) \tag{7}$$

λ, latent heat of vaporization (J g^{-1}); E, evaporation rate (g m^{-2} s^{-1}); α, P–T coefficient; s slope of the saturation vapor pressure curve (Pa C^{-1}); γ, psychrometric constant (Pa C^{-1}); R_n net radiation (W m^{-2}); G, ground heat flux (W m^{-2}).

The Priestley–Taylor coefficient, α, has been shown in numerous studies to have a mean value of 1.26 for potential evaporation from well-watered surfaces. Soil surfaces are only fully wet for a limited time following rainfall or irrigation, so it is inappropriate to use a constant value. Priestley and Taylor recognized this, and suggested that for bare soils α should be a function of the cumulative evaporation since the most recent rainfall or irrigation. Sttannard (1993) used this approach with an equation of the following form:

$$\alpha = 1.26 - \beta(1 - e^{-\mu\int E\,dt}) \tag{8}$$

We tried to fit this equation to eddy covariance measurements of evaporation from a bare soil at Rosemount, but found that it did not represent the initial stage following precipitation well. Eq. (8) implies that α begins to decline immediately following rewetting. Field data, though erratic immediately following rain, suggest that α remains at its potential value for some period of time before it begins to decline. This is consistent with the traditional concept of an energy-limited phase of soil evaporation (Jury et al., 1991). The field data were better described by the following equation, in which α_0, β, and μ are fitting coefficients, and cumulative evaporation since the last precipitation (E) is the independent variable.

$$\alpha = \alpha_0 - \frac{\beta}{1 + \exp(\mu - E)} \tag{9}$$

Eq. (9) describes a sigmoid function (Fig. 3), which illustrates the physical significance of the fitting parameters. The mean value of α for conditions when the surface is wet and evaporating at potential rates is α_0, and μ is the amount of evaporation, mm, that can be sustained before evaporation begins to decline. β represents the difference between α_0 and a minimum value of α that is asymptotically approached as the soil dries. For the silt loam at Rosemount, best fit to measured evaporative fluxes from bare soil was obtained with $\alpha_0 = 1.3$, $\beta = 0.9$, and $\mu = 5$ mm.

Net radiation is estimated from incoming solar radiation, air temperature, relative humidity, and leaf area index, with the aid

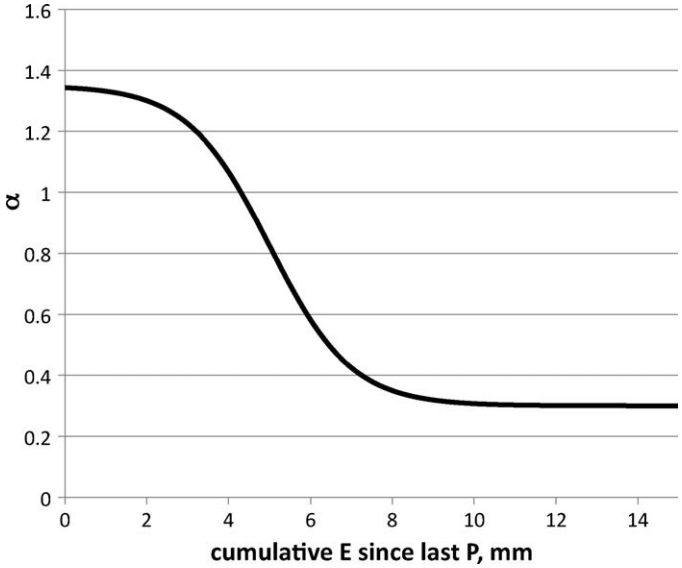

Fig. 3. Priestley–Taylor α for bare soil evaporation as a function of cumulative evaporation since the most recent rain. Open squares represent measured α, derived from flux measurements in spring 2006 at Rosemount, MN. Smooth curve shows the modeled α.

of a number of ancillary parameters, including latitude, longitude, and day of year. Solar radiation is compared with the calculated clear-sky radiation for the date and location in question to estimate the fraction of sky that is cloud-covered, which is in turn used to estimate an effective sky emissivity:

$$f_c = 1.35\left(1 - \frac{R_s}{R_{cs}}\right) \tag{10}$$

$$\varepsilon_{sky} = (1 - 0.84 f_c)\varepsilon_{cs} + 0.84 f_c \tag{11}$$

where ε_{cs} is the estimated clear sky emissivity corresponding to the ambient vapor pressure and humidity (Brutsaert, 1975):

$$\varepsilon_{cs} = 1.72\left(\frac{e}{T}\right)^{1.42} \tag{12}$$

Soil albedo and its dependence on surface wetness must be known or estimated. For the soil at our Rosemount, MN research site (Waukegan silt loam), wet albedo is 0.08 and when dry it is about 0.18. Albedo is scaled between these values in a manner analogous to the scaling of the Priestley–Taylor α, using the same parameters, on the premise that changes in wetness of the surface few mm are controlling both properties. The albedo of the rye is taken as 0.25, and the composite albedo is given by

$$r_{co} = r_{rye} - e^{(-1.5LAI)}(r_{rye} - r_{soil}) \tag{13}$$

Net radiation follows as

$$R_n = RS(1 - r_{co}) + (\varepsilon_{sky} - \varepsilon_{surf})\sigma T^4 \tag{14}$$

The energy available at the soil surface is the net radiation minus the energy consumed in transpiration:

$$R_{ns} = R_n - \lambda T \tag{15}$$

Soil evaporation is then estimated as

$$E_s = \alpha \frac{s}{s+\gamma}(R_{ns} - G) \tag{16}$$

where α is evaluated with Eq. (9). The soil heat flux, G, is taken to be a fixed fraction of R_{ns}, a simplification that is only supportable in an average sense, but suitable for our purposes. Evaluation of energy balance data over bare soils at our Rosemount site yielded a mean ratio of G/R_{ns} of about 0.25.

2.5. Soil moisture

We have foregone full-scale simulation of soil water flow. In the northern USA, Canada, and northern Europe, where much of the world's rye is grown, the winter cereal growing season is interrupted by freezing and thawing, and both snowfall and snowmelt are important hydrologic components. Mechanistic simulation requires simultaneous solution of heat and water flow, and in some cases consideration of overburden potentials, heaving and slumping (ONeill and Miller, 1985). These are non-trivial problems that substantially increase input data requirements and model complexity. For our purposes, a much simpler approach has been taken in which cumulative transpiration and evaporation are compared to cumulative precipitation to estimate soil moisture depletion. The primary goal is not to simulate rye response to water stress but to examine the potential impact of a winter rye cover crop on the subsequent grain crop. To do that, soil evaporation and water balance of a fallow site are simulated concurrently with the rye simulation, and the difference between the two is taken as an approximation of the hydrologic impact of the rye crop. We assume an effective rooting zone of 50 cm (Sainju et al., 1998; Vos et al., 1998), and a water content intermediate between the drained upper limit and the wilting point at the time of seeding. For a typical silt loam for instance, with a drained upper limit of 0.36 $m^3\,m^{-3}$ and a wilting point of 0.18 $m^3\,m^{-3}$, the

Fig. 4. Sites of weather stations providing data for the winter cover crop simulations.

simulation begins with 90 mm of available water in the profile. No attempt has been made to impose drought limitations on photosynthesis or transpiration; rather, any periods when soil moisture may be limiting are flagged to indicate likely diminution of production for a given set of hydrologic properties.

2.6. Assimilate partitioning

The model is not explicitly designed to predict yield or phenology, but in order to adequately predict biomass accumulation and water use it is necessary to partition assimilate between leaves, stems, reproductive structures, and roots with some measure of reality. There is a massive body of literature devoted to the observation and simulation of phenological development of cereal grains (see McMaster, 1997, for a thorough review). Much of it focuses on wheat, but the general concepts also apply to cereal rye (Wilhelm and McMaster, 1995). While there are many complicating factors, it is generally accepted that developmental staging proceeds as a function of accumulated thermal time, or growing degree-days (GDD). Some models explicitly "grow" wheat plants, with a specified number of degree-days needed to generate each leaf (Hay and Porter, 2006). This model operates at a lower level of complexity. We assume that the respective fractions of roots, leaves, stems, and grain that comprise total biomass are reasonably reproducible functions of cumulative GDD that can be numerically differentiated to partition fresh assimilate throughout the growing season. To apply this approach, we subdivided weekly samples of rye biomass from 2006 into leaves, stems, and reproductive parts to determine the fractions of each. These were then plotted against cumulative GDD, and logistic functions were developed to mimic the plots. Since root samples were unavailable, we used reported literature values of root/shoot ratios (Winzeler et al., 1989) to estimate root partitioning. Leaf mass and leaf area are inter-converted using a specific leaf area for rye of 25 $m^2\ kg^{-1}$ (Winzeler et al., 1989).

2.7. PAR beneath a senescing corn canopy

To model the emergence and growth of rye that has been aerially seeded into a corn canopy it is necessary to estimate the PAR available beneath the canopy. Measurements of both direct and diffuse PAR, above and below the canopy, were made in a corn field at Rosemount, MN in the late summer and fall of 2007, using line quantum sensors equipped with shadow bands. The resulting data were fit to a simple regression:

$$\tau = C_1 - C_2(t_h - t) \quad (17)$$

where τ is canopy transmittance, t is time (day), t_h is day of harvest, C_1 is the transmittance at the time of harvest (0.25), and C_2 is the slope of the regression (0.003).

2.8. Application of the model

Initially the model was run for five winter cereal seasons, 2002–2003 through 2006–2007, for several sites across the Midwestern United States where agricultural weather stations are sited, chosen to approximately span the climatic range of the corn belt (Fig. 4). For each site, harvest dates and planting dates for both corn and soybeans were estimated from data compiled by the National Agricultural Statistics Service (www.nass.usda.gov). The model was then run with a range of rye seeding dates for each site and year. Key outputs were the fractional cover at the cessation of fall growth, total biomass production at different spring harvest dates, soil moisture depletion, and corresponding water use relative to a

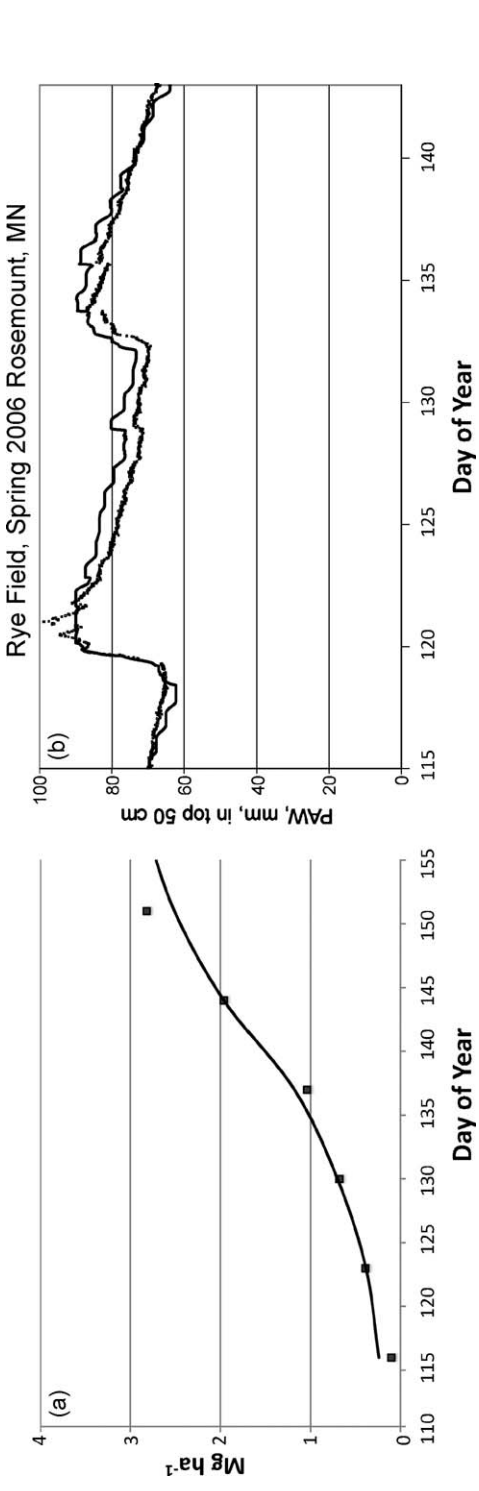

Fig. 5. (a) Measured (■) and modeled rye biomass accumulation, Rosemount, MN, 2006. (b) Measured (○) and modeled plant-available water in the surface 50 cm, Rosemount, MN, 2006.

parallel fallow (bare soil) simulation. The same soil properties, those of a typical silt loam soil, were used for all sites.

As the model algorithms were developed they were tested with meteorological data from the University of Minnesota Rosemount Research and Outreach Center, where winter rye was grown in the fall-spring interval between corn and soybeans in 2003–2004 and 2005–2006. This field is instrumented with an eddy covariance tower for measurement of net ecosystem exchange of CO_2 and H_2O (Baker and Griffis, 2005), along with various ancillary measurements, and is a part of the Ameriflux network of CO_2 flux measurement sites (http://public.ornl.gov/ameriflux/). A comparison of model estimates with measured values of biomass accumulation is shown in Fig. 5, along with a comparison of measured versus modeled plant-available water (PAW) in the upper 50 cm of soil.

3. Model results

Fig. 6 summarize the model estimates of rye biomass if it is produced conventionally, i.e. – planted with a grain drill after fall corn harvest and removed prior to spring planting of either corn (top panel) or soybeans (bottom panel). For each site the vertical solid bar represents the mean yield over 5 years with moderate N fertility (V_m = 80 μmol m^{-2} s^{-1}) and the shaded bar represents the high fertility case (V_m = 95 μmol m^{-2} s^{-1}). The latter would likely require significant additional N, while the former is probably closer to current practice, in which the rye is expected to grow on whatever residual N may be present following corn production. In fact, this is one of the primary cited attributes of rye (Kaspar et al., 2007; Strock et al., 2004) – its ability to remove the excess N that is an almost inevitable side effect of high-yielding corn production

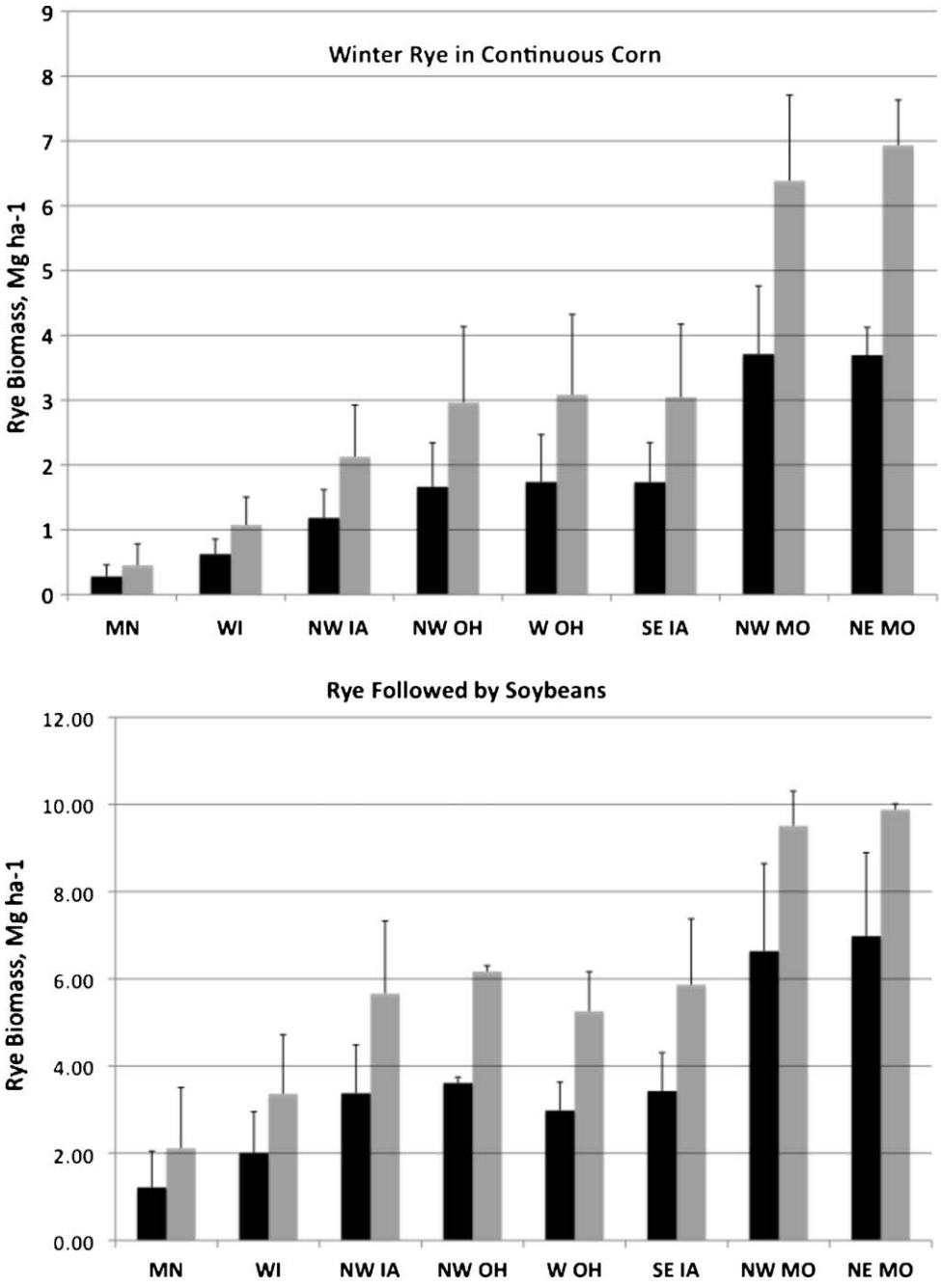

Fig. 6. 5-Year mean predicted rye biomass production in continuous corn systems (top panel) and corn–soybean systems (bottom panel), assuming rye is planted immediately after fall corn harvest and killed immediately before spring planting of the following crop.

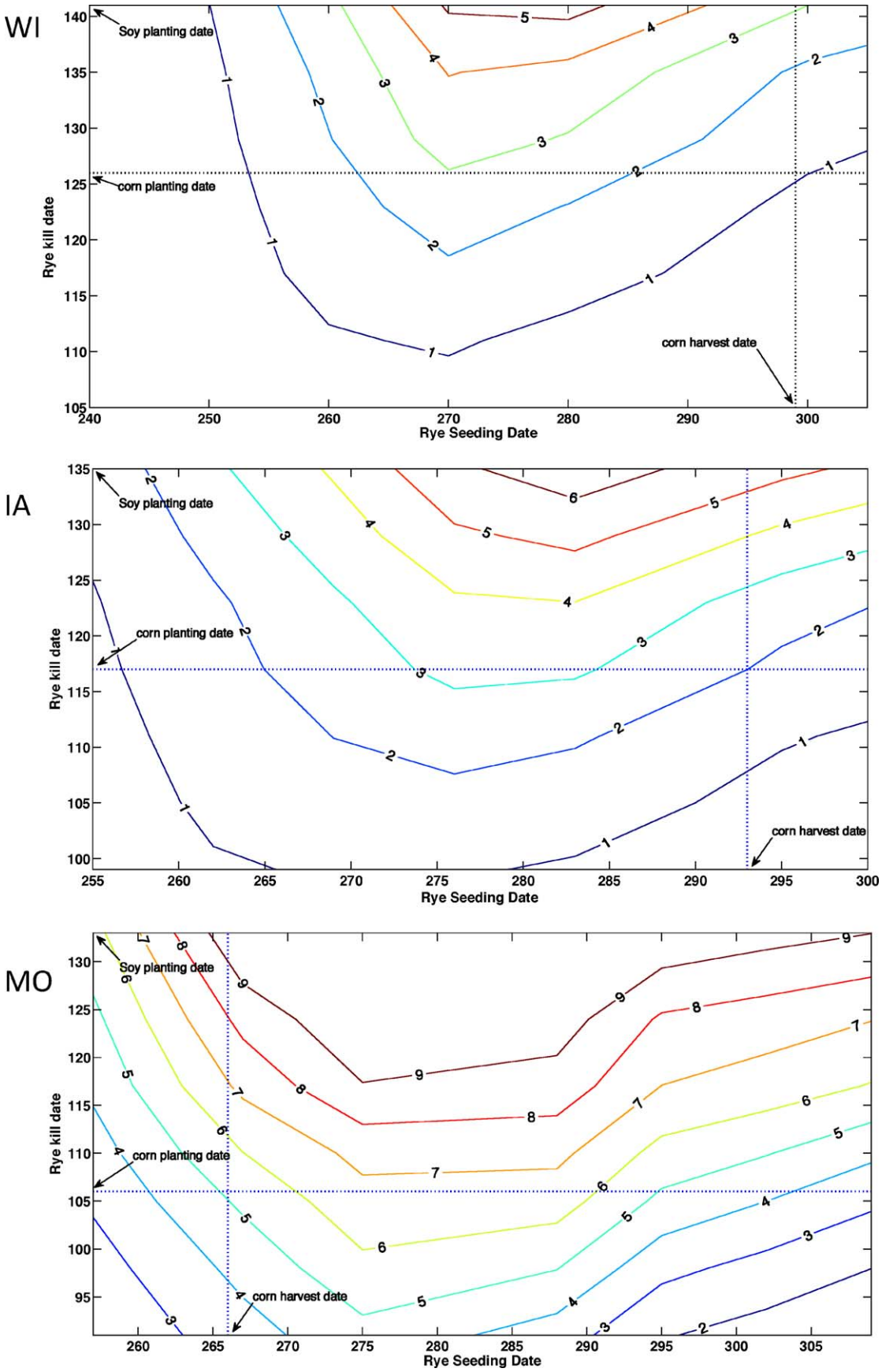

Fig. 7. Contour plots of estimated rye biomass production as a function of planting and harvest dates. The dashed vertical line indicates the date of fall corn harvest and the horizontal dashed line indicates the date of spring corn planting, while the upper *x*-axis in each plot denotes the date of spring soybean planting. Planting dates prior to corn harvest assume aerial seeding.

Table 1
Site coordinates and weather data. GDD refers to the cumulative growing degree-days during the rye growing season for each site, from fall emergence to the latest possible kill dates, taken as the mean planting dates for corn and soybeans. PAR is the cumulative PAR received during the same period for each site.

Location	Latitude	Longitude	GDD, *c*	GDD, *sb*	PAR, *c* (mol m^{-2})	PAR, *sb* (mol m^{-2})
MN	44.72N	93.05W	365 ± 128	606 ± 184	1136 ± 329	1788 ± 371
WI	43.338N	89.377W	390 ± 86	576 ± 105	1309 ± 290	1811 ± 386
W. IA	42.072N	95.913W	509 ± 68	732 ± 98	1517 ± 152	2141 ± 191
E. IA	41.416N	91.071W	650 ± 76	890 ± 76	1689 ± 213	2298 ± 189
NW MO	40.33N	94.42W	1013 ± 103	1389 ± 65	2381 ± 95	3223 ± 213
NE MO	40.013N	92.207W	1109 ± 62	1482 ± 72	2782 ± 104	3681 ± 427
NW OH	41.285N	83.844W	607 ± 76	816 ± 50	1656 ± 176	2237 ± 85
W OH	39.863N	83.672W	710 ± 69	939 ± 43	1712 ± 167	2242 ± 77

and a primary cause, together with excess phosphorus, of hypoxia in the Gulf of Mexico (Turner and Rabalais, 2003). Whether it makes economic sense to apply the extra N necessary for maximum rye biomass production depends on the cost of N, the yield response curve for rye, and the price that a currently non-existent biomass energy industry might pay. Environmental issues must also be considered. The growing season for winter cover crops is the prime period for ground water recharge in the main corn production region of the USA, so fertilizer application carries the risk of additional nitrate loading to ground water. For this reason, best management practices (BMPs) in most of the region specifically discourage fall N applications. Additional N inputs might also have negative atmospheric consequences; Crutzen et al. (2008) have concluded that the fraction of applied N that ultimately returns to the atmosphere as N_2O is much higher than IPCC estimates that are based on in-field measurements, due to subsequent offsite denitrification of NO_3^-. Ultimately, these losses must be better understood and properly factored into life-cycle analyses of any proposed biofuel production systems.

Fig. 7 contains a series of contour plots for selected site–years, in which potential rye biomass accumulation is plotted against fall seeding date and spring kill, or harvest, date. In each case, the upper horizontal axis represents the latest possible rye harvest, dictated by the mean soybean seeding date for the given site and year. The dashed horizontal line is the mean corn seeding date, and the vertical dashed line is the mean corn harvest date for the previous fall, when the rye was seeded. Thus, the lower right quadrant represents what is possible in a continuous corn rotation with conventional seeding practices, where the rye is not planted until the corn is removed and it is killed prior to corn planting the following spring. Similarly, the area to the right of the vertical dashed line encompass what is possible with standard seeding of rye following corn and removal prior to soybean planting. The area to the left of the vertical dashed line represents what could be possible with aerial seeding of the rye into standing corn prior to harvest.

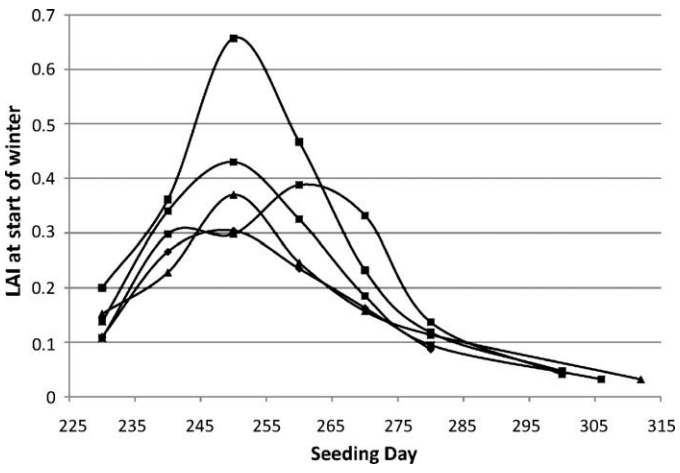

Fig. 8. Leaf area index at the conclusion of fall growth as a function of planting date for the Arlington, WI site. Each curve represents a separate year, and for each year the final data point represents planting on the day after corn harvest. All preceding data points for each year assume aerial seeding into a standing corn canopy.

There appears to be a clear benefit to aerial seeding for the MN and WI sites, a modest benefit in some years for the OH and IA sites, and no benefit for the MO sites, although the extent to which these conclusions are true depends on the validity of our assumptions regarding the efficacy (% emergence) of aerial seeding – there are scant data, mainly anecdotal, on the subject. Optimum timing of seeding varies from year-to-year at each site, but some general observations are possible. For all sites there is a penalty for aerially seeding too early. Phenological development of winter cereals is primarily driven by thermal time, embodied in the phyllochron concept (Wilhelm and McMaster, 1995; Hay and Porter, 2006). This implies a finite thermal lifetime and indeed there is evidence that the cumulative GDD from emergence to physiological maturity is relatively constant for rye (Nuttonson, 1957). However, biomass accumulation depends primarily on accumulated intercepted PAR during vegetative growth. Since the annual temperature cycle lags the solar cycle by approximately a month, the ratio of PAR to degree-days, and hence PAR per phyllochron, is generally greater in the spring than in the fall. This is exacerbated by aerial seeding, since the standing corn canopy further diminishes the PAR available for the rye crop beneath it. Thus the predicted yield reduction from seeding too early results from the rye spending too much time in the warm, low irradiance environment beneath a senescing corn canopy. At sites where there is an apparent aerial seeding benefit, the highest biomass yields are generally associated with seeding about 30–40 days prior to corn harvest, which allows time for germination, emergence, and a small amount of vegetative growth prior to winter. This is particularly important for the MN and WI sites, where both the total PAR and the degree-days available between fall corn harvest and spring soybean planting are quite a bit lower than the other sites (Table 1). Aerial seeding can also increase the LAI at the time of fall freeze-up (Fig. 8), particularly for the northernmost sites, where typically there is little time for rye to do much more than emerge if it is planted after corn harvest.

Not surprisingly, potential rye biomass production following corn and preceding soybean is much greater than it is in a continuous corn system. In most of the corn/soybean production region, soybeans are planted approximately 2 weeks later than corn. Those 2 weeks occur during a time when irradiance and temperature are typically optimal for rye growth, so if it is still in the vegetative stage a considerable amount of additional growth is possible. Of course, this is a time of high evaporative demand, raising the question of the water cost of rye biomass and its impact on the subsequent grain crop.

3.1. Water use

Model estimates of mean plant-available water remaining in the surface 50 cm of a typical silt loam soil following rye harvest

are shown in Fig. 9. In every case, water depletion is higher for the high V_{max} (high N) than for the low V_{max} simulation, consistent with the higher biomass production. Year-to-year variability is also greater for the high N simulations, indicative of greater risk associated with the greater potential reward. The Missouri locations and the NW Ohio site tended to show the greatest soil moisture depletion, but there were only two sites – the Missouri locations – and 1 year where available water was exhausted by the rye. This is not so surprising, since rye grows during the recharge portion of the hydrologic year in the Midwestern US. Precipitation during this period typically exceeds the storage capacity of the root zone by a substantial margin. In fact, more than 20 million ha of land in the corn belt have been drained in some way to remove excess water in the spring. Excepting Wisconsin, the percentage of cropland that is artificially drained in each state ranges between 25 and 60% (Zucker and Brown, 1998).

Comparisons of conventional row crop systems with adjacent native perennial areas have shown substantially more drainage from the agricultural system (Brye et al., 2000), and it has been suggested that the original conversion of native vegetation to cultivated crops probably caused an increase in base flow of rivers in the region (Twine et al., 2004). Widespread adoption of practices such as winter cover cropping that extend the 'transpirational season' could partially reverse this, and might be hydrologically beneficial in areas where spring planting and early season growth are frequently limited by excess soil moisture.

Conversely, although the model results suggest only modest reductions in total root zone PAW for most sites and years, even that could often have a negative impact on the germination and emergence of the succeeding crop, particularly if the rye-induced depletion is primarily confined to the near-surface seed zone. These effects can be reduced by earlier killing of the rye; such decisions could be made with the aid of medium term (5–7 days) precipitation forecasts. For example, killing the rye 1 week prior to soybean harvest at Castana IA in 2005 would save 20 mm of soil moisture, albeit at a cost of 1.5 t ha^{-1} of rye biomass (Fig. 10). Of course, all of these soil-moisture depletion results would be more serious on coarser-textured soils with lower water-holding

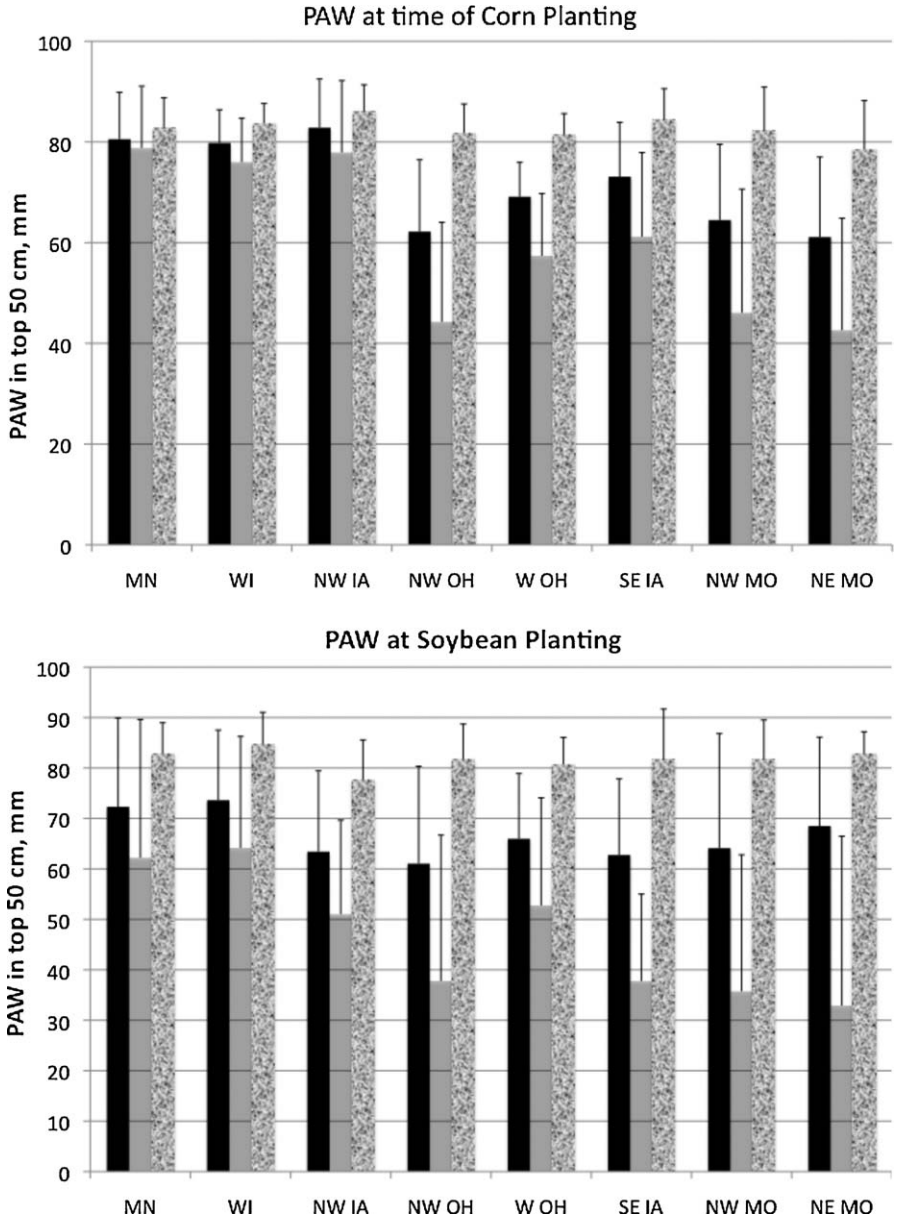

Fig. 9. Plant-available water remaining at the time of spring planting in corn/rye/corn systems (top panel) and corn/rye/soybean systems (bottom panel), for rye with moderate N content (V_m = 80, solid bars), rye with high N content (V_m = 95, gray bars), and no rye cover crop (bare soil, textured bars).

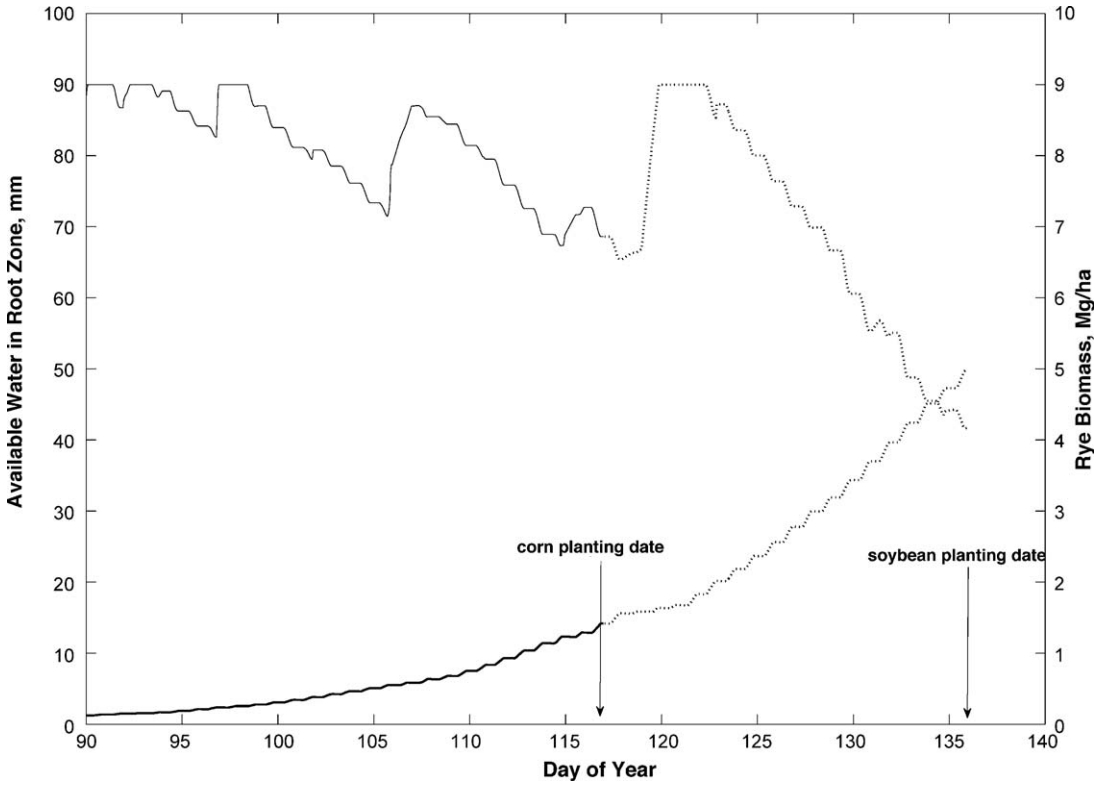

Fig. 10. Time series of model estimates of plant-available water and rye biomass for Western IA, 2005. Heavier solid line is rye biomass, lighter solid line is plant-available water in the root zone. In both cases, dashed lines indicate continuation past the time of corn planting, terminating at the time of soybean planting.

capacity. Corn and soybean production on such soils is already more frequently affected by drought, a situation that would be exacerbated by a winter-cover crop. However, any extra income potential from the biomass of a winter cover crop might tip the calculus in favor of installing irrigation on soils where producers have already been considering it.

The issue of economics is beyond the scope of this work, and is difficult to address since there is not yet a market for biomass. However, a few observations are possible. In assessing the potential for harvesting corn stover as a biofuel source, Graham et al. (2007) estimated the costs of harvesting, baling, and delivering stover to the farm gate, including the cost of nutrient replacement. Those collection costs, per Mg, are estimated as \$45 Mg^{-1} at a yield of 1 Mg ha^{-1}, decreasing asymptotically toward approximately \$20 Mg^{-1} at a yield of 9 Mg ha^{-1}. Average stover yields are approximately 6.5 Mg ha^{-1}, but it is neither physically possible nor environmentally sustainable to harvest it all. Wilhelm et al. (2007) have estimated the amount of residue that must be retained to prevent erosion and maintain soil organic carbon levels. This varies substantially with soil type and topography, but it has been estimated that about 30% of total corn stover produced nationally could be safely harvested at a cost of approximately \$33 Mg^{-1} (Graham et al., 2007). Harvest costs for rye stover would presumably be similar, but the cost of planting it must also be added in, unlike corn where those costs are already assigned to the grain. Currently, the cost of planting a rye cover crop ranges from \$20 to 30 ha^{-1}, depending on the method and rate of seeding. Consequently, the cost of delivering each Mg of rye biomass to the gate depends on both the method of seeding and the yield, ranging from a low of perhaps \$45–50 Mg^{-1} for a high-yielding, conventionally planted crop to a high in the vicinity of \$75 Mg^{-1} for a low-yielding, aerially seeded crop. Clearly rye cannot compete directly with corn as a biomass fuel source. A more likely role is as a "carbon supplement" to corn and corn–soybean systems; i.e. – the extra carbon input and erosion protection from the rye cover crop might allow a higher level of sustainable corn stover removal.

3.2. Uncertainties

Winter rye has historically been regarded as a low-value crop, so it has been the subject of comparatively little research. More information on the photosynthetic performance of rye, particularly at low temperature and as a function of leaf N status, would almost certainly improve the accuracy of the model in estimation of biomass accumulation. Similarly, the conclusions regarding the efficacy of aerial seeding must be regarded as highly speculative in the absence of more quantitative and comprehensive data. Finally, there is the question of cold-season impacts on rye development and phenology. We have made no attempt to simulate the vernalization process, since its primary impact is on flowering and grain yield, but it likely affects photosynthate partitioning and hence biomass accumulation. Also, in the absence of relevant data, we have been forced to assume that winter-kill is insignificant, which may not always be the case.

4. Conclusions

We have used a simple, robust model to estimate potential biomass production from a winter rye cover crop in continuous corn and corn–soybean systems at eight locations across the Midwestern US. The results indicate that this could provide 1–8 Mg ha^{-1} of additional biomass annually. The potential productivity is proportional to total available PAR and GDD during the period between fall corn harvest and spring planting, thus the lower amounts correspond to the northernmost locations in MN and WI. Aerial seeding of rye into standing corn may help, though not dramatically. The two southwestern-most locations, in MO,

consistently exhibited the highest *potential* production, but the associated soil water depletion would keep this potential from being consistently realized in the absence of supplemental irrigation. The intermediate sites in IA and OH, may provide the most stable performance, with moderate biomass yields and correspondingly less risk of a moisture-depleted root zone for the following corn or soybean crop.

Acknowledgements

Support for this project was provided by the USDA-ARS Renewable Energy Assessment Project (REAP) and the Office of Science (B.E.R.), U.S. Department of Energy, grant DE-FG02-03ER63684.

Appendix A. Modeling stomatal conductance in rye.

Leaf level assimilation rates were measured over a range of PAR intensities from 20 to 1000 μmol m^{-2} s^{-1}, at five different vapor pressure deficits ranging from 0.8 to 2.0 kPa. Measurements were made with a leaf chamber (LI-6400, Licor Inc., Lincoln, NE) on the uppermost fully expanded leaf. At any given *vpd* there was a clear relationship between c_i/c_s and PAR (Fig. A1), with the value approaching 1 as PAR decreased toward zero, and approaching a minimum as PAR increased, with the asymptotic limit inversely related to *vpd*. The dependence of the minimum on *vpd* was pronounced between 1.2 and 1.9 kPa, and flat outside that range.

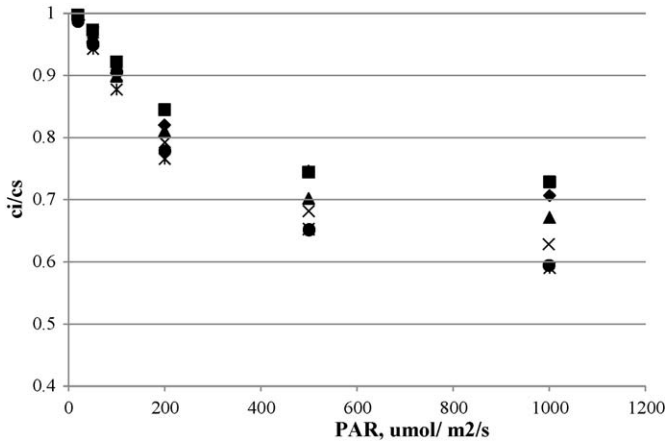

Fig. A1. Dependence of normalized internal CO_2 mole fraction (c_i/c_s) on PAR at six different vapor pressure deficits, ranging from 0.9 kPa (■) to 2.0 kPa (*).

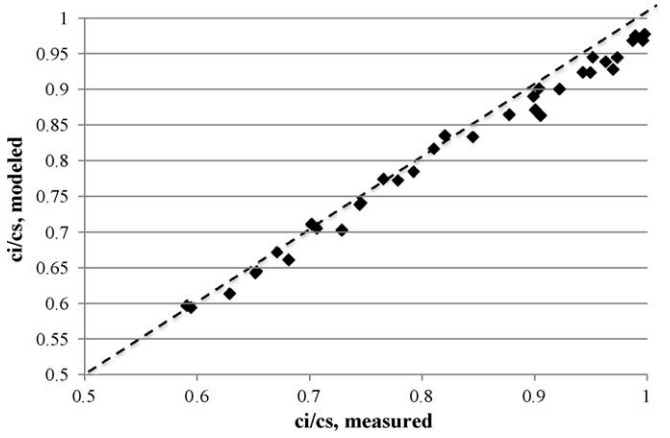

Fig. A2. Modeled versus measured c_i/c_s.

These relationships were fit to the following equations:

$$\varepsilon_{\min} = a - \frac{b}{1 + \exp(c - d\,vpd)}$$

$$\varepsilon = \varepsilon_{\min} + (1 - \varepsilon_{\min})\frac{PAR}{e}$$

$\varepsilon = c_i/c_s$; *vpd* = vapor pressure deficit (kPa); PAR = photosynthetically active radiation (μmol m^{-2} s^{-1}).

The fitting coefficients have the following values: $a = 0.7$, $b = 0.115$, $c = 16$, $d = 10$ kPa^{-1}, and $e = 250$ μmol m^{-2} s^{-1}. A scatter plot of modeled versus measured c_i/c_s is shown in Fig. A2. The agreement is quite acceptable, with only a slight deviation as c_i/c_s approaches unity, which has little consequence since this corresponds to very low PAR intensities. The universality of these relationships remains a matter for further exploration.

References

Anon, 2008. State of the climate in 2007. Bull. Am. Meteorol. Soc. 89 (7), 10.

Baker, J.M., Griffis, T.J., 2005. Examining strategies to improve the carbon balance of corn/soybean agriculture using eddy covariance and mass balance techniques. Agric. For. Meteorol. 128 (3/4), 163–177.

Baldocchi, D., 2008. Breathing of the terrestrial biosphere: lessons learned from a global network of carbon dioxide flux measurement systems. Aust. J. Bot. 56 (1), 1–26.

Brutsaert, W., 1975. On a derivable formula for long-wave radiation from clear skies. Water Resour. Res. 11 (742–744), 742.

Brye, K., Norman, J., Bundy, L., Gower, S., 2000. Water-budget evaluation of prairie and maize ecosystems. Soil Sci. Soc. Am. J. 64 (2), 715–724.

Campbell, G.S., Norman, J.M., 1998. Introduction to Environmental Biophysics, vol. xxi. Springer, New York, p. 286.

Coelho, B., Roy, R., Bruin, A., 2005. Long-term effects of late-summer overseeding of winter rye on corn grain yield and nitrogen balance. Can. J. Plant Sci. 85 (3), 543–554.

Collatz, J.G., Ball, J., Grivet, C., Berry, J., 1991. Physiological and environmental regulation of stomatal conductance, photosynthesis and transpiration- A model that includes a laminar boundary layer. Agric. For. Meteorol. 54 (2–4), 107–136.

Crutzen, P., Mosier, A., Smith, K., Winiwarter, W., 2008. N_2O release from agro-biofuel production negates global warming reduction by replacing fossil fuels. Atmos. Chem. Phys. 8 (2), 389–395.

dePury, D., Farquhar, G., 1999. A commentary on the use of a sun/shade model to scale from the leaf to a canopy. Agric. For. Meteorol. 95 (4), 257–260.

dePury, D., Farquhar, G., 1997. Simple scaling of photosynthesis from leaves to canopies without the errors of big-leaf models. Plant Cell Environ. 20 (5), 537–557.

Feyereisen, G., Sands, G., Wilson, B., Strock, J., Porter, P., 2006a. Plant growth component of a simple rye growth model. Trans. ASABE 49 (5), 1569–1578.

Feyereisen, G., Wilson, B., Sands, G., Strock, J., Porter, P., 2006b. Potential for a rye cover crop to reduce nitrate loss in southwestern Minnesota. Agron. J. 98 (6), 1416–1426.

Graham, R., Nelson, R., Sheehan, J., Perlack, R., Wright, L., 2007. Current and potential US corn stover supplies. Agron. J. 99 (1), 1–11.

Hay, R., Porter, J., 2006. The Physiology of Crop Yield. Blackwell, Oxford, UK, p. 314.

Jury, W.A., Gardner, W.R., Gardner, W.H., 1991. Soil Physics. John Wiley & Sons, New York, p. 328.

Kaspar, T., Jaynes, D., Parkin, T., Moorman, T., 2007. Rye cover crop and garnagrass strip effects on NO3 concentration and load in tile drainage. J. Environ. Qual. 36 (5), 1503–1511.

Kim, S.D., Dale, B.E., 2005. Life cycle assessment of various cropping systems utilized for producing biofuels: bioethanol and biodiesel. Biomass Bioenergy 29, 426–439.

Leuning, R., 1995. A critical appraisal of a combined stomatal-photosynthesis model for C-3 plants. Plant Cell Environ. 18 (4), 339–355.

McCree, K.J., 1974. Equations for the rate of dark respiration of white clover and grain sorghum as functions of dry weight, photosynthetic rate, and temperature. Crop Sci. 14 (4), 509–514.

McMaster, G., 1997. Phenology, development, and growth of the wheat (*Triticum aestivum* L.) shoot apex: a review. Adv. Agron. 59, 63–118.

Norman, J.M., 1993. Scaling processes between leaf and canopy levels. In: Ehleringer, J.R., Field, C.B. (Eds.), Scaling Physiological Processes: Leaf to Globe. Academic Press Inc., San Diego.

Nuttonson, M.Y., 1957. Rye–Climate Relationships and the Use of Thermal and Photo-thermal Requirements of Rye. American Institute of Crop Ecology, Washington, DC, p. 219.

ONeill, K., Miller, R., 1985. Exploration of a rigid ice model of frost heave. Water Resour. Res. 21 (3), 281–296.

Pacala, S., Socolow, R., 2004. Stabilization wedges: solving the climate problem for the next 50 years with current technologies. Science 305 (5686), 968–972.
Priestley, J.H.B., Taylor, R.J., 1972. On the assessment of surface heat flux and evaporation using large-scale parameters. Month. Weath. Rev. 100, 81–92.
Prince, S.D., Haskett, J., Steininger, M., Strand, H., Wright, R., 2001. Net primary production of U.S. Midwest croplands from agricultural harvest yield data. Ecol. Appl. 11, 1194–1205.
Ruffo, M., Bullock, D., Bollero, G., 2004. Soybean yield as affected by biomass and nitrogen uptake of cereal rye in winter cover crop rotations. Agron. J. 96 (3), 800–805.
Russelle, M., Morey, R., Baker, J., Porter, P., Jung, H., 2007. Comment on "Carbon-negative biofuels from low-input high-diversity grassland biomass". Science 316, 5831.
Sainju, U., Singh, B., Whitehead, W., 1998. Cover crop root distribution and its effects on soil nitrogen cycling. Agron. J. 90 (4), 511–518.
Schmid, H.P., Grimmond, C.S.B., Cropley, F., Offerle, B., Su, H.-B., 2000. Measurements of CO_2 and energy fluxes over a mixed hardwood forest in the mid-western United States. Agric. For. Meteorol. 103 (4), 357–374.
Strock, J.S., Porter, P.M., Russelle, M.P., 2004. Cover cropping to reduce nitrate loss through subsurface drainage in the northern U.S. Corn Belt. J. Environ. Qual. 33, 1010–1016.
Sttannard, D., 1993. Comparison of Penman–Monteith, Shuttleworth–Wallace, and modified Priestley–Taylor evapotranspiration models for wildland vegetation in semiarid rangeland. Water Resour. Res. 29 (5), 1379–1392.
Tilman, D., Hill, J., Lehman, C., 2006. Carbon-negative biofuels from low-input high-diversity grassland biomass. Science 314 (5805), 1598–1600.
Turner, R., Rabalais, N., 2003. Linking landscape and water quality in the Mississippi river basin for 200 years. Bioscience 53 (6), 563–572.
Twine, T., Kucharik, C., Foley, J., 2004. Effects of land cover change on the energy and water balance of the Mississippi River basin. J. Hydromet. 5 (4), 640–655.
Vos, J., van der Putten, P., Hussein, M., van Dam, A., Leffelaar, P., 1998. Field observations on nitrogen catch crops. II. Root length and root length distribution in relation to species and nitrogen supply. Plant Soil 201 (1), 149–155.
Wilhelm, W., McMaster, G., 1995. Importance of the phyllochron in studying development and growth in grasses. Crop Sci. 35 (1), 1–3.
Wilhelm, W.W., Johnson, J.M.F., Karlen, D.L., Lightle, D.T., 2007. Corn stover to sustain soil organic carbon further constrains biomass supply. Agronomy Journal 99, 1665–1667.
Winzeler, M., McCullough, D., Hunt, L., 1989. Leaf gas exchange and plant growth of winter rye, triticale, and wheat under contrasting temperature regimes. Crop Sci. 29 (5), 1256–1260.
Wong, S., Cown, I., Farquhar, G., 1979. Stomatal conductance correlates with photosynthetic capacity. Nature 282 (5737), 424–426.
Yu, Q., Liu, Y., Liu, J., Wang, T., 2002. Simulation of leaf photosynthesis of winter wheat on Tibetan Plateau and in North China Plain. Ecol. Modell. 155 (2–3), 205–216.
Zucker, L.A., Brown, L.C., 1998. Agricultural Drainage. Series 2000b, Bull. 871. The Ohio State University, Columbus, OH, p. 40.